

The Effect of Seeding Method on The Growth of Zinc Oxide Nanorods

Yasmin.Z¹, M. I. Idris^{1,2*}, H.H.M Yusof¹, Z. A. F. M. Napiyah^{1,2}, M. Rashid³, M.N. Shah Zainudin¹, H. Zainuddin⁴

¹ Fakulti Kejuruteraan Elektronik & Kejuruteraan Komputer, Universiti Teknikal Malaysia Melaka (UTeM), Hang Tuah Jaya, 76100 Durian Tunggal, Melaka, Malaysia.

² Micro and Nano Electronic (MiNE), Centre for Telecommunication Research and Innovation (CeTRI), Fakulti Kejuruteraan Elektronik & Kejuruteraan Komputer, Universiti Teknikal Malaysia Melaka (UTeM), Hang Tuah Jaya, 76100 Durian Tunggal, Melaka, Malaysia.

³ School of Physics, Universiti Sains Malaysia (USM) 11800, Pulau Pinang, Malaysia

⁴ Fakulti Kejuruteraan Elektrik, Universiti Teknikal Malaysia Melaka (UTeM), Hang Tuah Jaya, 76100 Durian Tunggal, Melaka, Malaysia.

Received 27 May 2022, Revised 30 June 2022, Accepted 5 July 2022

ABSTRACT

The paper presents the investigation of the method of seeding process for the growth of zinc oxide (ZnO) nanorods (NRs) on the glass substrate as an electron transport layer (ETL) for solar cells. The ZnO NRs were grown by using the hydrothermal method. The seeding process was done via average deposition of zinc crystallite on the glass surface, and the process was compared between with and without spin coating technique. The effect of spin coating parameters during seeding phase on the growth of ZnO nanorods was also investigated in this study. It was found that the sample prepared using the unfiltered solution without spin coating in the seeding phase exhibited the densest ZnO NRs layer with the highest absorption coefficient and high crystallinity.

Keywords: Zinc Oxide, Nanorods, Nanostructure, Spin Coating, Hydrothermal, Electron Transport Layer

1. INTRODUCTION

Solar power is one of the renewable resources that are widely used in the world. There has been a renewed interest in the harvesting of solar radiation using photovoltaics. For example, dye-sensitized solar cell (DSSC) comprises a dye-sensitized photoanode and an electrolyte separated counter electrode in the third generation of solar cells (CE). Photons intercepted by the dye-monolayer produce excitons that are instantly dispersed into the conduction band of the ETL at the nanoparticle surface. A promising strategy to improve the electron transport layer (ETL) in solar cells is to replace the photoelectrode of nanoparticles with single-crystalline nanoparticles. It provides a large internal surface area. Nanorods (NRs) are nanomaterial classes with unique optical, magnetic, electrical, and mechanical properties, which is an appealing choice for multiple applications [1]. NRs also provides a unique opportunity to explore the remarkable physical properties of all nanostructures [2]. Nanostructured zinc oxide (ZnO) can be fabricated using various thin film techniques such as spray pyrolysis [3], sputtering [4], metal-organic chemical vapor deposition [5], and hydrothermal process [6]. The hydrothermal method is widely adopted for the fabrication of transparent and conducting oxide as the simplicity, reliability without involving an expensive vacuum system and indeed a cheap way for large area coating. Other benefits are provided by the hydrothermal method, such as better control over the morphology

and the size of the synthesized materials [7], ease of management, and low-cost thin-film fabrication of chemical components elucidate the structure and optical properties of ZnO NRs [8]. Among the possible methods to acquire the ZnO NRs, the hydrothermal growth process is lean to

idzdihar@utem.edu.my

low-cost and ideal for large-scale development. [9]. For the large-scale development of ZnO NRs, the hydrothermal method is the most comfortable and economical [10].

The structure of ZnO is hexagonal wurtzite (lattice constant $a = 0.3249$ nm, $c = 0.5206$ nm) [11], a versatile substance with wide-ranging applications [12]. It can be considered as a multifunctional material because of its unique physical and chemical properties. ZnO is a semiconductor of the n-type II-VI compound [13] with a broad bandgap of 3.37 eV. Although DSSC based on ZnO generally produces lower conversion efficiency than TiO₂ in DSSC, it remains a possible alternative [14] due to high charge carrier (electron) mobility, transparent to visible light advantageous in morphology. It has attracted intensive research effort because of its unique properties and versatile applications.

Moreover, ZnO is interesting to be developed due to its high position of the conduction band, which allows the possibility to generate higher photovoltage. There are many other factors for the incredible popularity of ZnO, such as having enormous exciton binding energy (~60 meV) leads to excitons that exist at room temperature [15], excellent thermal stability [16], high mechanical and high chemical intensity. The thin film can be synthesized and developed by different techniques [17]. Several studies have shown that ZnO NRs are regulated by several important parameters such as aqueous solution acidity (pH), precursor concentration, growth time, growth temperature, type of seed layer, and seed layer thickness [18]. Much attention has been drawn to the nanostructured ZnO materials due to their specific properties [19]. Previous studies have shown that ZnO discovers large application areas such as planar nano due to its greater surface area, which ZnO favors catalytic properties [20]. Thus, ZnO thin films may play a significant role in developing advanced materials [21].

In this work, ZnO NRs were fabricated onto the glass surface via the hydrothermal method, and their morphology and optical properties were studied in terms of the number of spin-coating cycles (number of repetitions for spin coating and heat treatment) and rotational speed of the spin coater affecting the roughness and thickness of the seed layer. The molar ratio of the starting solution, formation duration, formation temperature, refreshing solution, seed layer thickness, and annealing temperature are other considerations that could affect the diameter and length of the NRs.

2. EXPERIMENTAL WORK

2.1 Sample Cleaning Process

The research work includes the glass cleaning process, the synthesis of ZnO NRs, and optoelectronic characterizations of ZnO NRs. The synthesis of ZnO nanostructures such as nanowires, nanocycles, nanobelts, and nanocombs has been achieved successfully over the past ten years [22]. In this work, to synthesize ZnO nanostructures utilized a hydrothermal process. The hydrothermal synthesis method involves one of the various techniques to crystallize substances [23]. The process desires the temperature differential between the opposite ends of

the crystallizing compartment to be continuously preserved. Two phases were involved in this fabrication process, which is the seeding phase and growth phase.

Initially, the glasses were cleaned using a standard process before the seeding phase. The glass dimension is 76.2 mm (L) by 25.4 mm (W) with 1.2 mm glass thickness. Before the synthesis of ZnO NRs began, the glass cleaning process took place. At first, the glasses were cut using a diamond cutter into the size of 20 mm by 15 mm according to the measurement of the spin coater for the glass. Next, all the glasses were washed with liquid detergent and then transferred in the ethanol and sonicated to eliminate organic impurities for 15 minutes in isopropyl alcohol (IPA) while still wet. The glasses were rinsed and treated for 15 minutes with deionized (DI) water in the ultrasonic bath. The cleaned glasses were then eventually dried at 90 ° C in an oven to run dry without any water marks. Figure 1 summarized the flowchart of the ZnO NRs synthesis process onto the surface of the glass, including the seeding phase and the growth phase.

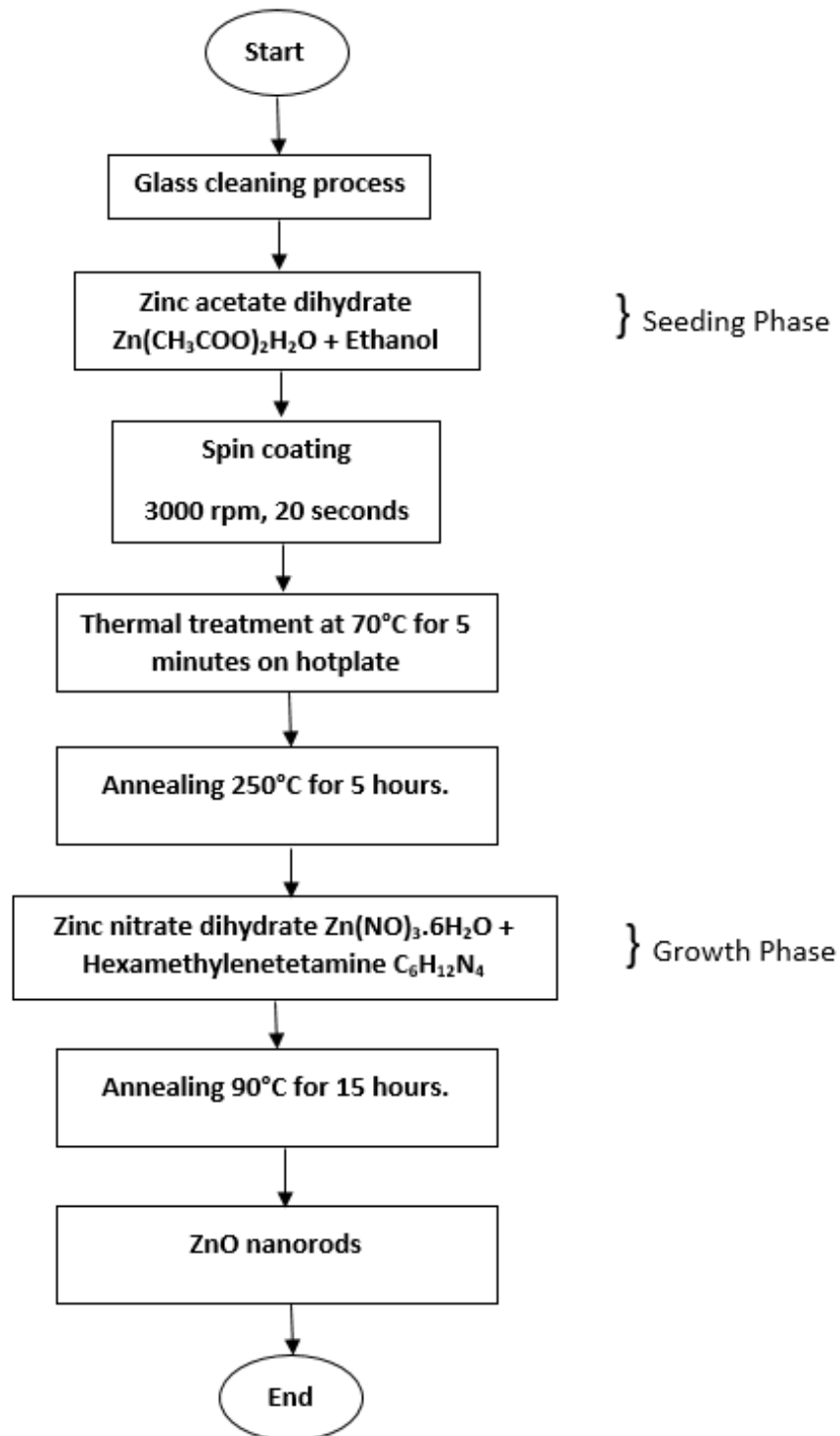


Figure 1. The flowchart of the ZnO NRs synthesis process onto the surface of the glass, including the seeding phase and the growth phase.

2.2 Seeding Process

The seed layer is an essential factor in growing vertically aligned ZnO NRs as the thickness of the seed layer affects the resulting alignment and morphology of ZnO NRs. The seed layer plays a significant role in the growth of high-quality NRs as the prominent role to the high surface area of the glass substrate. The preparation of a high-quality seed layer is an essential step toward developing the performance of nanostructures [24]. Figure 2 shows the crucial steps in the seeding process.

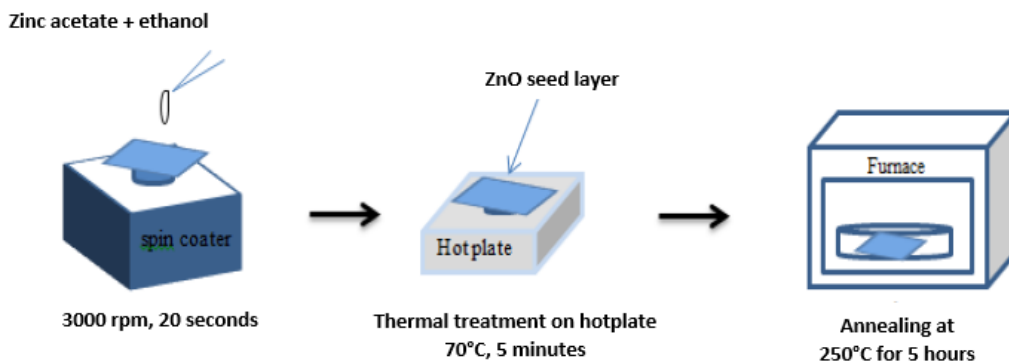


Figure 2. The seeding phase for the growth of NRs using spin coating technique followed by thermal and annealing treatment.

The seeding phase took place after the glass cleaning process, where the mixture of zinc acetate dihydrate ($\text{Zn}(\text{CH}_3\text{COO})_2 \cdot 2\text{H}_2\text{O}$, Sigma Aldrich) and ethanol dissolved completely with constant stirring on the hot plate at 60–65°C. During the seeding process, an amount of seeding solution was dropped on the glass surface and spin-coated at a spinning speed of $v = 3000$ rpm for 20 seconds. The samples were spin-coated according to the rotational speed (v) and the number of spin cycles (n) that has been set in the spin coating parameter, as shown in Table 1. The drying process on a hotplate followed the process maintained at 70°C for 5 minutes. The procedure was repeated according to the parameter that has been set to obtain the thickness of the ZnO thin films. Finally, the ZnO seed layer was annealed for 5 hours at 250°C. In this experimental work, there were five samples of ZnO NRs with different numbers of cycles and spin coating, as shown in Table 1 took place. Based on the spin coating parameter in Table 1, the spin coating varies in type of solutions and methods. Unfiltered solution (sample a,b,c and e) did not undergo the filtration process, while filtered solution (sample d) underwent the filtration process by using filter paper to observe the difference between these two solutions. - Meanwhile, samples d and e were prepared by drop-casting the solution onto the glass surface without using a spin coater.

Table 1 The spin coating parameter of ZnO NRs on the seeding process according to the number of cycles and spin coating process.

Sample	Spin Coating Parameter	
	No of Cycle (n)	Spin Coating
a	10	Yes(unfiltered solution)
b	20	Yes(unfiltered solution)

c	30	Yes(unfiltered solution)
d	10	No (filtered solution)
e	10	No (unfiltered solution)

2.3 Growth Process

The growth process is a process to grow NRs from the seeding phase to form the crystalline shape and length of NRs. In the stage of NRs growth, the growth solution of ZnO NRs was prepared by using the mixture of 10 mM of zinc nitrate hexahydrate ($Zn(NO_3)_6 \cdot 6H_2O$, QReC) and hexamethylenetetramine (HMTA) ($C_6H_{12}N_4$, Sigma Aldrich) in 400 ml of deionized (DI) water. The seeded glasses were placed facing down with a 2mm thickness of holder (glass substrate) to ensure enough gap between the bottom surface of a beaker and the glass, as shown in Figure 3.

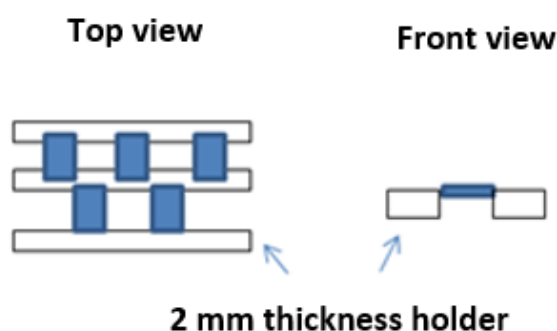


Figure 3. Top view and front view of the position of the samples in the growth process.

The seeded glasses were then immersed entirely in the growth solution and kept in an Ecocell oven at $90^\circ C$ for 15 hours, as shown in Figure 4. During the growth process, A new precursor solution was regularly replaced with 100 ml of growth solution every 5 hours to maintain a constant growth rate of ZnO NRs to prevent chemical degradation during the growth process. Upon completion, the samples were retracted from the growth solution and thoroughly rinsed with DI water several times.

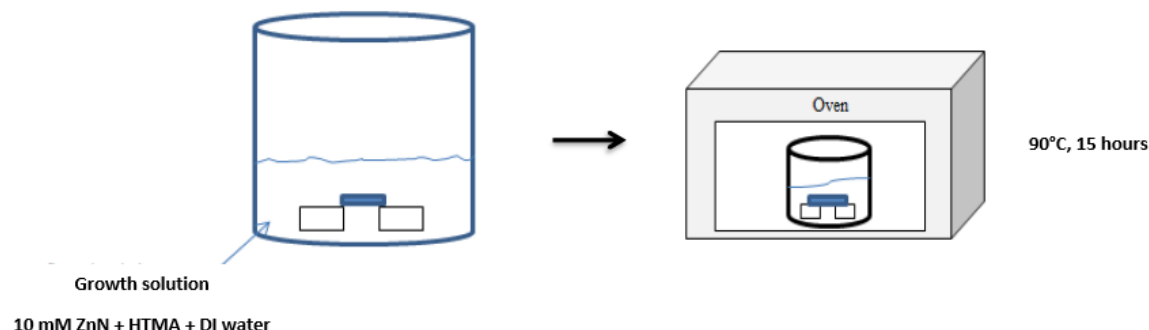


Figure 4. The process of the growth phase in the growth solution for 15 hours at $90^\circ C$ in the oven.

The substrate was dried at room temperature after the NRs were grown. The scanning electron microscope (SEM) images were taken to analyze the ZnO NRs. X-ray Diffraction (XRD) profiles were carried out to study the crystallinity of the seed layers and NRs, followed by UV-Vis spectroscopy (UV-Vis). Figure 5 showed one of the final samples of ZnO NRs has a white coating on the glass after all the experimental work has been done.

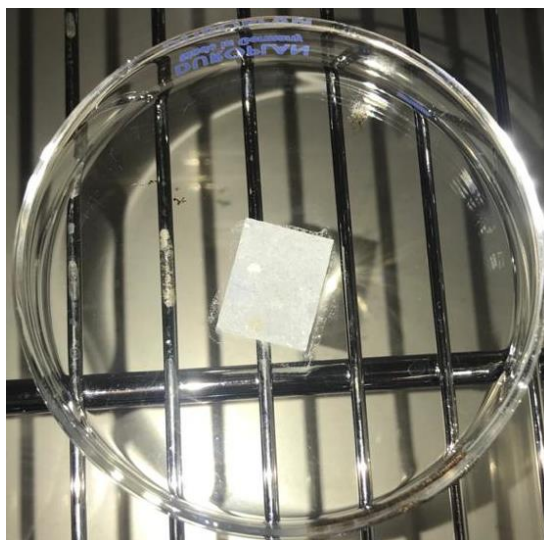


Figure 5. The final sample of the growth of ZnO NRs after undergoing the seeding phase and growth phase.

3. RESULTS AND DISCUSSION

Scanning Electron Microscope (SEM)

The surface morphologies of ZnO NRs were analyzed using SEM micrographs (20 kx) of the ZnO NRs for all samples, as shown in Figure 6. A clear formation of NRs structures was observed for all samples except for sample d, as shown in Figure 6(d), in which the solution was filtered before the seeding process. It is believed that the concentration of zinc acetate was reduced after was filtered and thus resulted in poor quality of the seed layer. The samples with a different number of cycles for the spin coating as in Figure 6(a), 6(b), and 6(c) did not show a significant difference in NRs density. On the other hand, the sample in Figure 6(e) (unfiltered solution without spin coating) exhibited the densest of ZnO NRs compared to the different samples. The crystallinity of the NRs in the vertical direction provides the boost for the length of the NRs.

The SEM images of ZnO NRs grown on the different number of cycles for the spin coating resulted in the average length of ZnO NRs at different seed layer thicknesses. The increase in seed layer thickness seems to have only slightly affected the average length of ZnO NRs, (Fig. 6(a)-(e)) with and without spin coating technique. This is due to the ZnO NRs growth on all ZnO seed layer thicknesses has a small difference in lengths. However, the alignment for ZnO NRs with spin coating and without resulted not well aligned but high in size and low diameter NRs. The spin coating method affects the spreading of the seed layer on the glass substrate, but it is possible to adjust the size of ZnO NRs when the immersion time is varied at a fixed concentration. Alterations can regulate the size of the ZnO NRs in the immersion time at a given concentration.

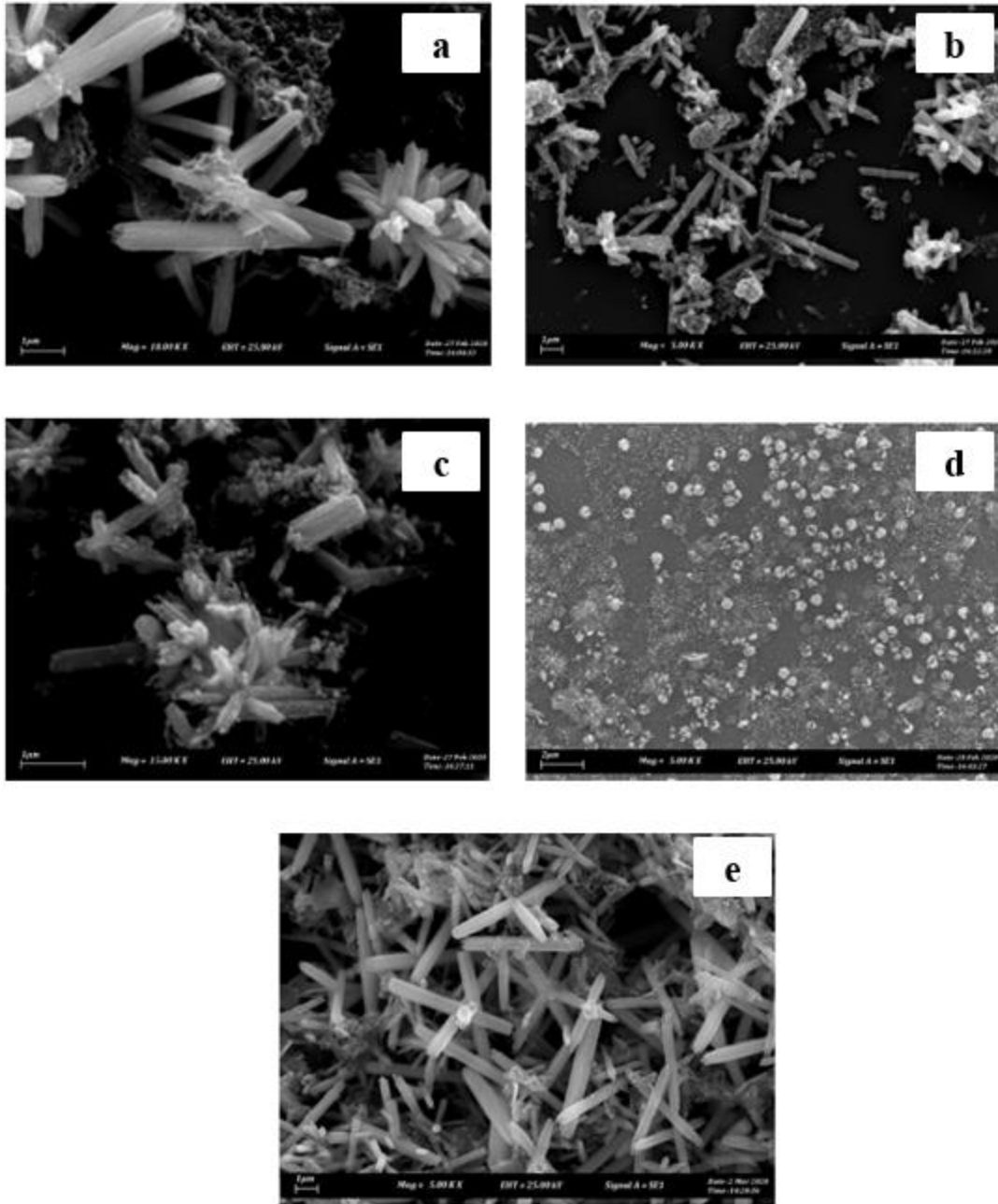


Figure 6. The SEM images of ZnO NRs for $v = 3000$ RPM at n values of: (a) 10 cycles, (b) 20 cycles, and (c) 30 cycles and no spin coating at n values of: (d) 10 cycle with filtered solution, (e) 10 cycles unfiltered solution.

X-Ray Diffraction (XRD)

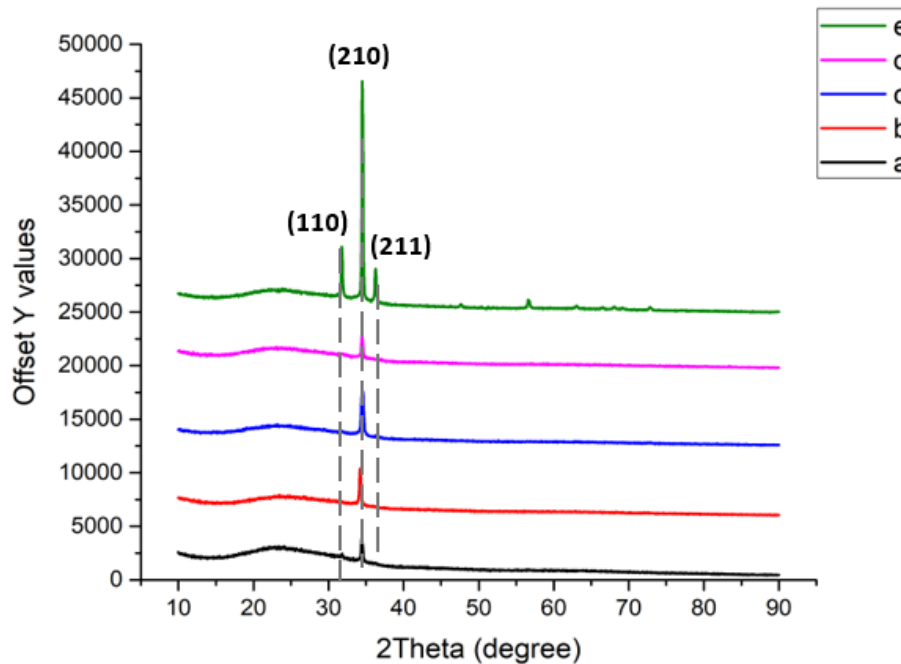


Figure 7. X-ray diffraction pattern of the ZnO NRs for samples a,b,c,d, and e, respectively.

Figure 7 shows the graph of ZnO NRs XRD patterns obtained from the XRD analysis, where several peaks have been observed. The XRD patterns of the ZnO NRs show that three major peaks at $2\theta = 34.56^\circ$, $2\theta = 36.37^\circ$ and $2\theta = 63.19^\circ$ correspond to the diffraction from the $\langle 110 \rangle$, $\langle 212 \rangle$, and $\langle 211 \rangle$ planes, respectively. Sample e resulted in the highest peak intensity and electron density among the samples. The average crystal (diameter) of nanoparticles evaluated by the Scherrer equation [25]:

$$D = \frac{k\lambda}{\beta \sin \theta} \quad (1)$$

Where k is a structural constant, λ is the X-Ray wavelength (1.54060 \AA), d is the nanoparticle diameter, and β is full width at half maximum (FWHM), θ is the angle of Bragg. Consequently, the XRD characterization result makes it possible to conclude that the ZnO nanoparticles have an average diameter of around 11 nm. As shown in Table 2, FWHM comparisons indicate that the FWHM ($^\circ 2\theta$) decreased as the thickness of the ZnO seed layer increased. However, sample e shows that the crystallinity without the spin coating of the ZnO seed layer at ten cycles number thickness (unfiltered solution) is the maximum of these sample sets.

Table 2 The features of ZnO NRs by estimated XRD patterns.

No of Cycle (n)	FWHM (°2Th.)	d-spacing [Å]
a = 10	0.2598	1.91204
b = 20	0.1948	2.60435
c = 30	0.1624	2.59475
d = 10	0.0900	1.81527
e = 10	0.7793	2.80887

UV-Vis Spectroscopy

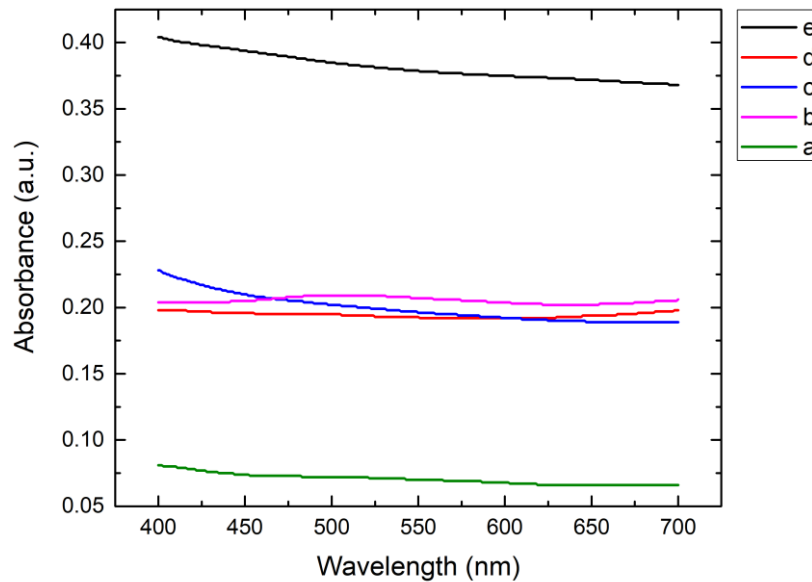


Figure 8. Respectively demonstrates the absorption spectra for samples a,b,c,d, and e at 400 - 700 nm wavelength.

This study aims to study the optical properties of the photovoltaic cells, especially the absorbance properties. Normally this study is performed from 200nm up to 100 nm wavelength. However, due to the noise at the ultraviolet range (200 to 300 nm), the graph illustrates visible wavelengths from 400-700 nm. The relationship in graph Figure 8 is between absorption and wavelength. Every sample has a different absorption peak of λ_{peak} . Hence, the dominant wavelength of light is absorbed. There were three primary absorption peaks for the visible wavelengths ranging from 400-700 nm for samples b, c, and d. Meanwhile, the UV-vis absorption for sample e exhibited the highest magnitude in the range 500-600 nm.

4. CONCLUSION

We have successfully demonstrated the growth of ZnO NRs onto the surface of the glass substrate by using the hydrothermal method. The effect of the seeding method on the structural properties was also investigated. The XRD analysis concluded that sample e has the highest peak intensity and crystallinity, with an average diameter of approximately 2 nm. These results are correlated with SEM and UV visible analysis where sample e exhibited the densest ZnO NRs layer and highest in the UV-vis absorption. To develop NRs, the smoothness and the seed density of the seed layer are very significant. The rotation speed (v) and the number of spin cycles (n) can regulate the smoothness and seed density of the seed layer. Therefore, to obtain a higher density of ZnO NRs, it is suggested to reduce the speed of spin coater and increase the number of the cycle (solution drop) during the seeding phase.

ACKNOWLEDGEMENTS

Project No supported this work of research. RACER/2019/FKEKK-CETRI/F00405 Micro & Nano Electronics (MiNe), Department of Faculty of Electronic Engineering & Computer Engineering, Universiti Teknikal Malaysia Melaka (UTeM) and by Universiti Sains Malaysia (USM) through Short Term Grant 304/PFIZIK/6315133.

REFERENCES

- [1] Yusof, H. H. M., Harun, S. W., Dimyati, K., Bora, T., Mohammed, W. S., & Dutta, J. (2018). Optical dynamic range maximization for humidity sensing by controlling growth of zinc oxide nanorods. *Photonics and Nanostructures - Fundamentals and Applications*, 30, 57–64.
- [2] Pokai, S., Limnonthakul, P., Horprathum, M., Eiamchai, P., Pattantsetakul, V., Limwicchan, S., ... Chitichotpanya, C. (2017). Influence of seed layer thickness on well-aligned ZnO nanorods via hydrothermal method. In *Materials Today: Proceedings* (Vol. 4, pp. 6336–6341). Elsevier Ltd.
- [3] Krunks, M. and Mellicov, E. (1995) Zinc Oxide Thin Films by the Spray Pyrolysis Method. *Thin Soled Filme*, 270, 33-36.
- [4] Nunes, P., Costa, D., Fortunate, E. and Martiens, R. (2002) Performenes Presented by Zinc Oxide Thin Films Deposited by R. F. Magnetron Sputtering. *Vacumm*, 64, 293-297.
- [5] Wu, J.-J. and Liu, S.-C. (2002) Low-Temperature Growth of Well-Aligned ZnO Nanarods by Chemical Vapor Deposition. *Advanced Materials*, 14, 215-218.
- [6] Ni, Y.H., Wei, X.W., Hong, J.M. and Ye, Y. (2005) Hydrothermal Synthesis and Optical Properties of ZnO Nanorods. *Materials Science and Engineering: B*, 121, 42-47.
- [7] Kale, R.B., Hsu, Y.J., Lin, Y.F., and Lu, SY (2014). Hydrothermal synthesis, characterizations and photoluminescence study of single crystalline hexagonal ZnO nanorods with three dimensional flowerlike microstructures. *Superlattices and Microstructures* 69, 239–252.
- [8] Kurda A. H.Hassan Y. M.Ahmed N. M. (2015) Controlling Diameter, Length and Characterization of ZnO Nanorods by Simple Hydrothermal Method for Solar Cells. *World Journal of Nano Science and Engineering*
- [9] Cesini, I., Kowalczyk, M., Lucantonio, A., D’alesio, G., Kumar, P., Camboni, D., Massari, L., Pingue, P., De Simone, A., Morgera, A.F., et al. (2020). Seedless hydrothermal growth of ZnO nanorods as a promising route for flexible tactile sensors. *Nanomaterials* 10.

- [10] Mbuyisa, P.N., Ndwandwe, O.M., and Cepek, C. (2015). Controlled growth of zinc oxide nanorods synthesised by the hydrothermal method. *Thin Solid Films* 578, 7–10.
- [11] Li, X., Chen, X., Yi, Z., Zhou, Z., Tang, Y., and Yi, Y. (2019). Fabrication of ZnO nanorods with strong UV absorption and different hydrophobicity on foamed nickel under different hydrothermal conditions. *Micromachines* 10.
- [12] Lin, K. F., Cheng, H. M., Hsu, H. C., Lin, L. J., & Hsieh, W. F. (2005). Band gap variation of size-controlled ZnO quantum dots synthesized by sol-gel method. *Chemical Physics Letters*, 409(4–6), 208–211
- [13] Chee, C.Y., Nadarajah, K., Siddiqui, M.K., and Wong, Y. (2014). Optical and structural characterization of solution processed zinc oxide nanorods via hydrothermal method. *Ceramics International* 40, 9997–10004
- [14] Bramantyo, Albertus & Poespawati, Nji & Kenji, Murakami. (2016). Optimization of ZnO seed layer for growth of vertically aligned ZnO nanorods on glass surface.
- [15] Hassanpour, A., Bogdan, N., Capobianco, J.A., and Bianucci, P. (2017). Hydrothermal selective growth of low aspect ratio isolated ZnO nanorods. *Materials and Design* 119, 464–469.
- [16] Iwan, S., Fauzia, V., Umar, AA, and Sun, XW (2016). Room temperature photoluminescence properties of ZnO nanorods grown by hydrothermal reaction. In *AIP Conference Proceedings*, (American Institute of Physics Inc.), p.
- [17] Omar, Azimah & Abdullah, Huda & Shaari, Sahbudin & Taha, Mohd. (2013). Characterization of zinc oxide dye-sensitized solar cell incorporation with single-walled carbon nanotubes. *Journal of Materials Research*. 28. 10.1557/jmr.2013.25.
- [18] Pokai, Supawadee & Limnonthakul, Puenisara & Horprathum, M. & Eiamchai, Pitak & Pattantsetakul, Viyapol & Limwichean, Saksorn & Nuntawong, Noppadon & Porntheeraphat, Supanit & Chitichotpanya, Chayanisa. (2017). Influence of seed layer thickness on well-aligned ZnO nanorods via hydrothermal method. *Materials Today: Proceedings*. 4. 6336-6341. 10.1016/j.matpr.2017.06.136.
- [19] Gao, S., Li, D., Li, Y., Lv, X., Wang, J., Li, H., Yu, Q., Guo, F., and Zhao, L. (2012). Growth and characterization of ZnO nanorod arrays on boron-doped diamond films by low temperature hydrothermal reaction. *Journal of Alloys and Compounds* 539, 200–204.
- [20] Emil, Elif & Alkan, Gözde & Gurmen, Sebahattin & Rudolf, Rebeka & Feizpour, Darja & Friedrich, Bernd. (2018). Tuning the Morphology of ZnO Nanostructures with the Ultrasonic Spray Pyrolysis Process. *Metals - Open Access Metallurgy Journal*. 8. 10.3390/met8080569.
- [21] Fudzi, L.M., Zainal, Z., Lim, H.N., Chang, S.K., Holi, A.M., and Ali, M.S.M. (2018). Effect of temperature and growth time on vertically aligned ZnO nanorods by simplified hydrothermal technique for photoelectrochemical cells. *Materials* 11.
- [22] Chen, C.C., Wu, T.L., Meen, T.H., Chen, C.Y., Su, C.H., Tsai, J.K., Lee, C.Y., Lee, C.H., and Liu, D.S. (2019). ZnO nanogenerator prepared from ZnO nanorods grown by hydrothermal method. *Sensors and Materials* 31, 1083–1089.
- [23] Sannakashappanavar, Basavaraj & Pattanashetti, Nandini & Reddy, Byrareddy & Yadav, Aniruddh. (2018). Study of annealing effect on the growth of ZnO nanorods on ZnO seed layers. *AIP Conference Proceedings*. 1943. 020077. 10.1063/1.5029653.
- [24] Hamza, Forat & Hassan, Zainuriah & Alrawi, Naser & Elfadill, Nezar & Abd, Husnen. (2018). Effects of ZnO seed layer thickness on catalyst-free growth of ZnO nanostructures for

enhanced UV photoresponse. *Optics & Laser Technology*. 98. 344-353.
10.1016/j.optlastec.2017.06.031.

- [25] Burton, Allen & Ong, Kenneth & Rea, Thomas & Chan, Ignatius. (2009). On the estimation of average crystallite size of zeolites from the Scherrer equation: A critical evaluation of its application to zeolites with one-dimensional pore systems. *Microporous and Mesoporous Materials*. 117. 75-90. 10.1016/j.micromeso.2008.06.010.